Human Cancer Biology

A Distinct Spectrum of Copy Number Aberrations in Pediatric High-Grade Gliomas

Dorine A. Bax[1], Alan Mackay[3], Suzanne E. Little[1], Diana Carvalho[1,6,7], Marta Viana-Pereira[1,6], Narinder Tamber[3], Anita E. Grigoriadis[4], Alan Ashworth[3], Rui M. Reis[6], David W. Ellison[8], Safa Al-Sarraj[5], Darren Hargrave[2], and Chris Jones[1,2]

Abstract

Purpose: As genome-scale technologies begin to unravel the complexity of the equivalent tumors in adults, we can attempt detailed characterization of high-grade gliomas in children, that have until recently been lacking. Toward this end, we sought to validate and extend investigations of the differences between pediatric and adult tumors.

Experimental Design: We carried out copy number profiling by array comparative genomic hybridization using a 32K bacterial artificial chromosome platform on 63 formalin-fixed paraffin-embedded cases of high-grade glioma arising in children and young people (<23 years).

Results: The genomic profiles of these tumors could be subclassified into four categories: those with stable genomes, which were associated with a better prognosis; those with aneuploid and those with highly rearranged genomes; and those with an amplifier genotype, which had a significantly worse clinical outcome. Independent of this was a clear segregation of cases with 1q gain (more common in children) from those with concurrent 7 gain/10q loss (a defining feature of adults). Detailed mapping of all the amplification and deletion events revealed numerous low-frequency amplifications, including *IGF1R*, *PDGFRB*, *PIK3CA*, *CDK6*, *CCND1*, and *CCNE1*, and novel homozygous deletions encompassing unknown genes, including those at 5q35, 10q25, and 22q13. Despite this, aberrations targeting the "core signaling pathways" in adult glioblastomas are significantly underrepresented in the pediatric setting.

Conclusions: These data highlight that although there are overlaps in the genomic events driving gliomagenesis of all ages, the pediatric disease harbors a distinct spectrum of copy number aberrations compared with adults. *Clin Cancer Res; 16(13); 3368–77. ©2010 AACR.*

The use of genome-scale profiling techniques to identify the key genetic aberrations underlying various tumor types has led to fundamental discoveries about the drivers of oncogenesis, and provides the rationale for specific targeted therapies in these lesions. Until recently, the application of such studies to the fields of high-grade glioma specifically,

Authors' Affiliations: [1]Section of Paediatric Oncology, The Institute of Cancer Research, and [2]Paediatric Oncology, Royal Marsden Hospital, Sutton, United Kingdom; [3]Breakthrough Breast Cancer Research Centre, The Institute of Cancer Research, and [4]Breakthrough Breast Cancer Unit and [5]Clinical Neuropathology, Kings College Hospital, London, United Kingdom; [6]Life and Health Sciences Research Institute, University do Minho, Braga, Portugal; [7]Center for Neuroscience and Cell Biology, University of Coimbra, Coimbra, Portugal; and [8]St Jude Children's Research Hospital, Memphis, Tennessee

Corresponding Author: Chris Jones, Section of Paediatric Oncology, Institute of Cancer Research, Sutton, Surrey, SM2 5NG, United Kingdom. Phone: 44-0-20-8722-4416; Fax: 44-0-20-8722-4321; E-mail: chris.jones@icr.ac.uk.

and childhood tumors in general, have lagged behind the adult epithelial cancers. This is now rapidly changing, with large screens of adult glioblastoma through collaborative networks (1) or single institutions (2) joining an increasing number of smaller independent studies (3–7) in comprehensively mapping the glioblastoma genome.

There are also beginning to emerge genomic studies specifically addressing childhood cancers, and there is mounting evidence that the pediatric high-grade glioma genome has certain key differences with that of histologically similar adult tumors. An early study using metaphase comparative genomic hybridization (CGH; ref. 8) highlighted distinct chromosomal changes in 23 childhood cases, a result borne out in a later 10K single nucleotide polymorphism (SNP) array study of a further 14 high-grade tumors (9), and more recent studies of 18 pediatric glioblastoma on Illumina 100K arrays (10), and 20 high-grade tumors using molecular inversion probes (11). Most recently, we participated in a collaborative effort to carry out molecular profiling of 78 pediatric high-grade gliomas by Affymetrix 500K SNP and U133 Plus2.0 expression arrays (12). From all these studies, it seems clear that although there are many large-scale chromosomal and

Translational Relevance

Pediatric high-grade gliomas represent clinically devastating and biologically understudied tumors of the central nervous system. Little is known about the key genomic alterations that arise in childhood cases, nor of the specific differences between these and the adult disease. We present the copy number profiling of a large series of these rare tumors, and identify numerous low-frequency events previously unreported in pediatric high-grade glioma, including the potential therapeutic target *IGF1R*. Tumors could be classified into distinct genomic subtypes, with marked differences in clinical outcome, and an idealized $PDGFRA^{amp}$, 1q+, 16q-genotype was considerably enriched in pediatric cases, in contrast to the $EGFR^{amp}$, 7+, 10q- cases more commonly associated with adults. We further highlight the importance of platelet-derived growth factor (PDGF) signaling in this context, through the most commonly observed genomic amplification of *PDGFRA*, as well as a unique amplification of *PDGFRB*, providing strong rationale for clinically targeting this pathway in children with this disease.

specific genetic amplification/deletion events common to tumors from patients of all ages, there are certain events found at significantly different frequencies in pediatric versus adult lesions.

One of the most immediately apparent differences was the high frequency of chromosome 1q gains and 16q losses, and the lower frequency of (often concurrent) gain of chromosome 7 and loss of 10q in childhood cases compared with adults. Although there were numerous low-frequency amplifications and deletions such as *MYC/MYCN*, *CCND2*, *KRAS*, and *CDKN2C*, which seemed to show the pediatric high-grade glioma genome to be similar to clinical secondary adult glioblastomas (13, 14), a lack of *IDH1* mutations in the childhood setting showed the distinct biological pathways active during pathogenesis (12).

The most common amplification in the pediatric cases was at 4q12, with shortest region of overlap (SRO) and expression analyses identifying the amplicon driver to be *PDGFRA* (12). This was present in up to 17% of primary pediatric glioblastoma, and 29% of diffuse intrinsic pontine glioma, and was also found in 50% of cases of high-grade glioma arising as a secondary malignancy after cranio-spinal radiation (post-IR). Many cases without *PDGFRA* amplification were still found to show overexpression of a specific *PDGFRA*-associated gene signature, which was itself distinct from that observed in adult cases with the 4q12 amplification. Taken together, platelet-derived growth factor (PDGF)-driven signaling seems to be preferentially activated in the majority of pediatric tumors, in contrast to adults, where epidermal growth factor receptor (EGFR) is implicated as the predominant target (12).

Although these studies are beginning to unravel the key features of the pediatric high-grade glioma genome, the total number of cases studied remains considerably smaller than for adult tumors. This is of particular importance given the lower frequency of the majority of genetic aberrations detected in childhood cases. Validating these low-frequency events in independent cohorts as being recurrent abnormalities, as well as the likely identification of novel isolated copy number changes will aid our understanding of the key pathways underlying the diversity of high-grade gliomas in children. To this end we carried out an array CGH study of 63 cases of pediatric high-grade glioma from formalin-fixed, paraffin-embedded (FFPE) archival pathology specimens on a 32K tiling-path bacterial artificial chromosome (BAC) platform.

Materials and Methods

Samples and DNA extraction

High-grade glioma samples from 63 patients (<23 years old) treated at the Royal Marsden Hospital (RMH), Sutton, and the Newcastle Royal Infirmary, United Kingdom, were obtained after approval by local and multicenter ethical review committees. The collection consisted of 37 glioblastoma multiforme, 14 anaplastic astrocytomas, 4 anaplastic oligodendrogliomas, 4 diffuse intrinsic (brain stem) gliomas, 2 astroblastoma, 1 oligoastrocytoma, and 1 gliosarcoma. All cases were archival FFPE tissues. The presence of tumor tissue in these samples and the tumor type were verified on a H&E-stained section independently by two neuropathologists (DWE and SA-S). Nine of the cases were previously profiled from a frozen tumor specimen in the collaborative SNP study (12). DNA was extracted using the DNeasy Tissue Kit (Qiagen) according to the manufacturer's protocol and quantitated on a NanoDrop spectrophotometer (Thermo Scientific).

Array CGH

All raw and processed data have been deposited in Array Express (http://www.ebi.ac.uk/microarray-as/ae/; E-TABM-857). The array CGH platform used in this study was constructed at the Breakthrough Breast Cancer Research Centre and comprises 31,619 overlapping BAC probes covering the human genome at an approximate resolution of 50 kb (A-MEXP-1734). Hybridizations were carried out as previously described (15) and slides were scanned using an Axon 4000B scanner (Axon Instruments) with images analyzed using Genepix Pro 4.1 software (Axon Instruments). The median localized background slide signal for each clone was subtracted and each clone Cy5/Cy3 ratio was normalized by local regression (loess) against fluorescence intensity and spatial location. Clones overlapping known copy number variants were removed for statistical and visualization purposes, but not for mapping of specific amplifications

and deletions, which was done according to the March 2006 build of the human genome sequence (hg18).

Data analysis

All data transformation and statistical analysis were carried out in R 2.9.0 (http://www.r-project.org/) and Bio-Conductor 2.4 (http://www.bioconductor.org/), making extensive use of modified versions of the package aCGH in particular (15). For identification of DNA copy number alterations, data were smoothed using a local polynomial adaptive weights procedure for regression problems with additive errors, with thresholds for assigning "gain" and "loss" set at 0.1 (3 × SD of control hybridizations). For visualization purposes, the processed log_2 ratios were colored green (gain) or red (loss) after segmentation and copy number determination.

To assess the significance of the genomic alterations, we applied an algorithm similar to those previously described, namely, Genomic Identification of Significant Targets in Cancer (GISTIC; ref. 13) and Genome Topography Scanning (GTS; ref. 16), taking into account the frequency, amplitude, and focality of the observed amplifications (log_2 ratio >1.0) and deletions (log_2 ratio <−0.75). This was calculated as the product of the absolute log_2 ratio, the number of clones in each segment, and the frequency within the entire cohort, scaled to the absolute maximum for amplifications/deletions separately, and overplotted on the frequency histogram for gains and losses described above.

Fluorescent *in situ* hybridization

Fluorescent *in situ* hybridization (FISH) analysis was carried out on FFPE sections as previously described (17). Probes directed against *MYCN* (pool of clones RP11-1183P10, RP11-674F13 and RP11-754G14), *PIK3CA* (RP11-4B14, RP11-642A13, RP11-379M20), *PDGFRA* (RP11-819D11, RP11-58C6), *SKP2* (RP11-749P08, CTD-2010F22), *PDGFRB* (RP11-211F05, RP11-21I20), *MYC* (RP11-440N18, RP11-237F24, CTD-2034C18), *CDK4* (RP11-66N19, RP11-277A02, RP11-672O16), *MDM2* (RP11-611O02, RP13-618A08, CTD-2067J14), and *IGF1R* (CTD-2015I17, RP11-203H14, RP11-189B22) were labeled with Cy3 (GE Healthcare), whereas chromosome-specific control probes at loci of no copy number change were labeled with fluorescein (GE Healthcare). Hybridized preparations were counterstained with 4′, 6-diamidino-2-phenylindole in antifade (Vector Laboratories Inc.). Images were captured using a cooled charge-coupled device camera (Photometrics).

Statistics

All statistical tests were done in R2.9.0. Correlations between categorical values were done using the χ^2 and Fisher's exact tests. Correlations between continuous variables were done using Student's t test or the Mann-Whitney U test. Cumulative survival probabilities were calculated using the Kaplan-Meier method on uniformly treated patients within our cohort from the same institution (RMH),

with differences between survival rates analyzed with the log-rank test. Important prognostic information (including extent of resection, Karnofsky performance score) was not available for all cases in this retrospective study, so multivariate analysis could not be done. All tests were two-tailed, with a confidence interval of 95%. P values of <0.05 were considered statistically significant.

Results

Distinct patterns of copy number change in the pediatric high-grade glioma genome

Previously we utilized whole genome amplification strategies for array CGH studies of tumors extracted from FFPE specimens (18). In this study, however, we were able to utilize a cohort of samples for which sufficient material was available to avoid the previous approach. We were able to generate high-quality copy number profiles from an unselected series of 63 pediatric high-grade gliomas using 32K tiling-path BAC arrays from which the tumor cell purity could be verified as >90% without the need for additional steps.

We observed a mean number of large-scale (whole chromosome or chromosomal arms) gains and losses of 5.8 per sample (median, 4; range, 0-22), with more losses (mean, 3.5; median, 3; range, 0-14) than gains (mean, 2.3; median, 2; range, 0-11). There was a further mean of 1.8 focal amplifications/deletions per sample (median, 1; range, 0-11), again with a slightly increased number of deletions (mean, 1.0; median, 0; range, 0-8) compared with amplifications (mean, 0.8; median, 0; range, 0-4). The list of observed alterations is given for the full dataset in Supplementary Table S1.

We were able to subtype the samples into four groups based upon the pattern of their genomic profiles. First was a group of tumors that had a very stable genome, with few (<3), low-level, focal changes. This subtype comprised 13 of 63 (20.6%) cases, and included 8 tumors (12.7%) that harbored no detectable copy number alterations on our 32K BAC platform (Fig. 1A). The second type contained only large, single copy alterations involving whole chromosomes or chromosomal arms, resulting in aneuploidy in the absence of any high-level amplifications in 22 of 63 (34.9%) cases, the largest subgroup we observed (Fig. 1B). The third type harbored numerous, low-level, intrachromosomal breaks resulting in multiple gains and losses and a highly rearranged genome. This group was also defined for this purpose by exclusion of cases with bona fide amplicons, and comprised 11 of 63 (17.5%) of the cohort (Fig. 1C). Finally, we considered those tumors with single or multiple high-level (log_2 ratio >1.0) amplifications, regardless of the genomic background, as belonging to the fourth, "amplifier" subtype. This group consisted of 17 of 63 (27.0%) of cases (Fig. 1D).

There were no significant correlations between genomic subtype and WHO grade or histology ($P > 0.05$, Fisher's exact test), with glioblastomas, anaplastic astrocytomas,
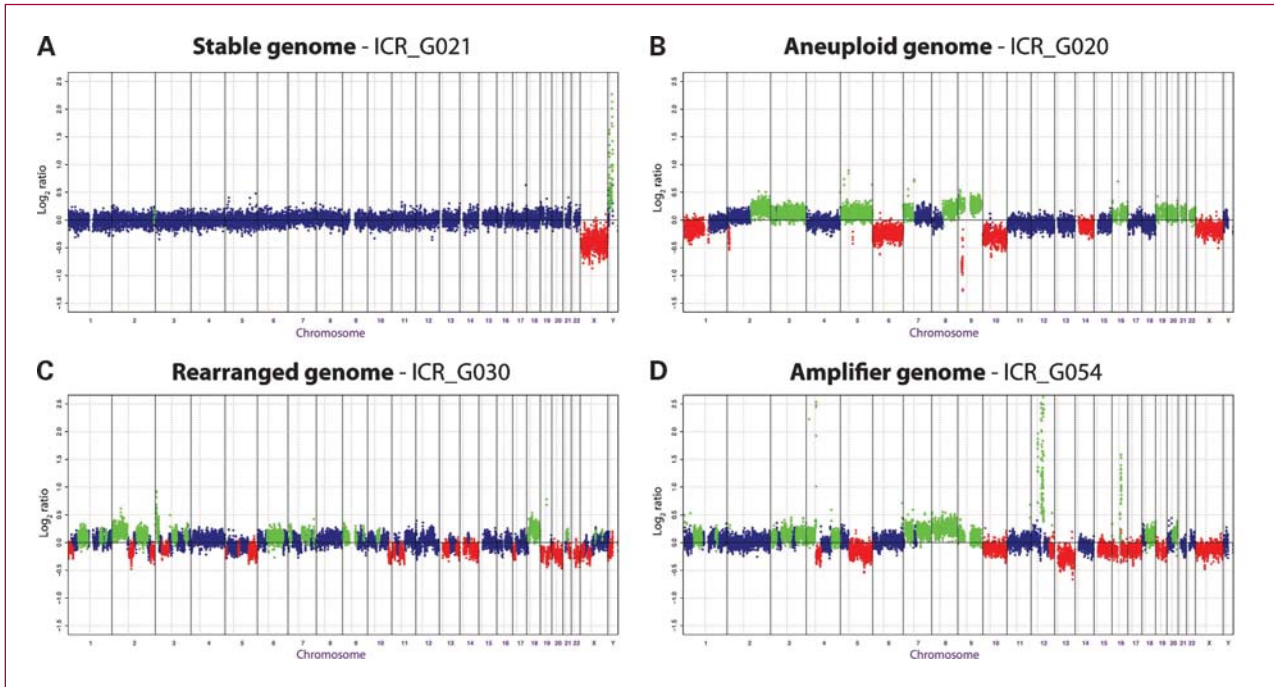
Fig. 1. Pediatric high-grade gliomas comprise different subtypes of copy number profiles. Sample genome plots are given for stable (A), aneuploid (B), rearranged (C), and amplifier (D) genomes within our sample cohort. Log_2 ratios for each clone (Y-axis) are plotted according to chromosomal location (X-axis). Vertical lines, centromeres; green points, gains; red points, losses.

and anaplastic oligodendrogliomas spread across all sub-types. Of note, there were no "stable" genomic cases among the series of five patients that were treated for a previous malignancy by cranio-spinal radiation (post-IR; Supplementary Table S1). There was also no association of copy number profiles with age at diagnosis ($P > 0.05$, Mann-Whitney U test), although the amplifier group did not include any infant tumors (<3 years). However, when

we investigated the overall survival of the patients treated at a single institution (RMH), we detected significant differences by retrospective univariate analysis in the clinical outcome of cases according to the genomic profile of the tumor. The stable genome cases showed a trend towards better prognosis when compared with all other cases ($P = 0.0755$, log-rank test), whereas the samples with an amplifier genome had a significantly shorter time to death

Fig. 2. Genomic subtypes of pediatric high-grade glioma have prognostic relevance. Kaplan-Meier plot for overall survival of pediatric high-grade gliomas treated at a single institution stratified according to genomic subtype. The stable genome cases showed a trend towards better prognosis when compared with all other cases ($P = 0.0755$, log-rank test), whereas the samples with an amplifier genome had a significantly shorter time to death ($P = 0.00214$, log-rank test).
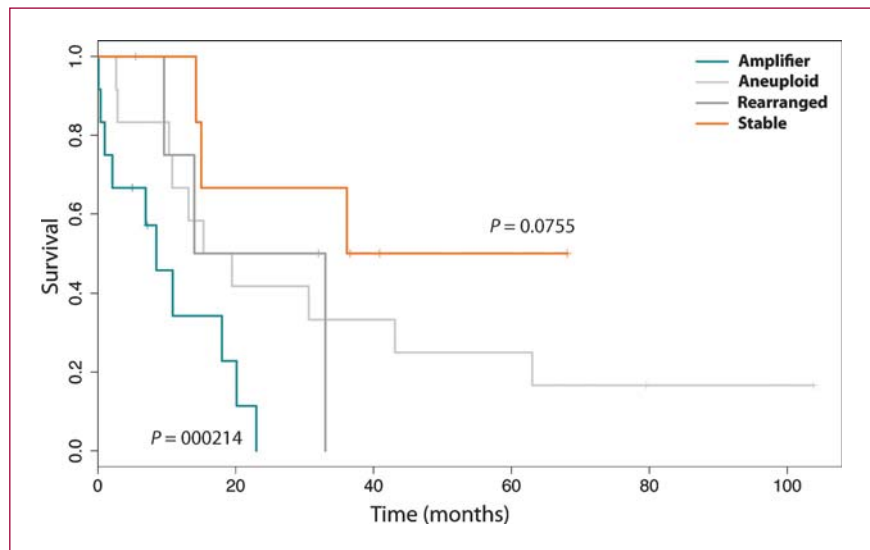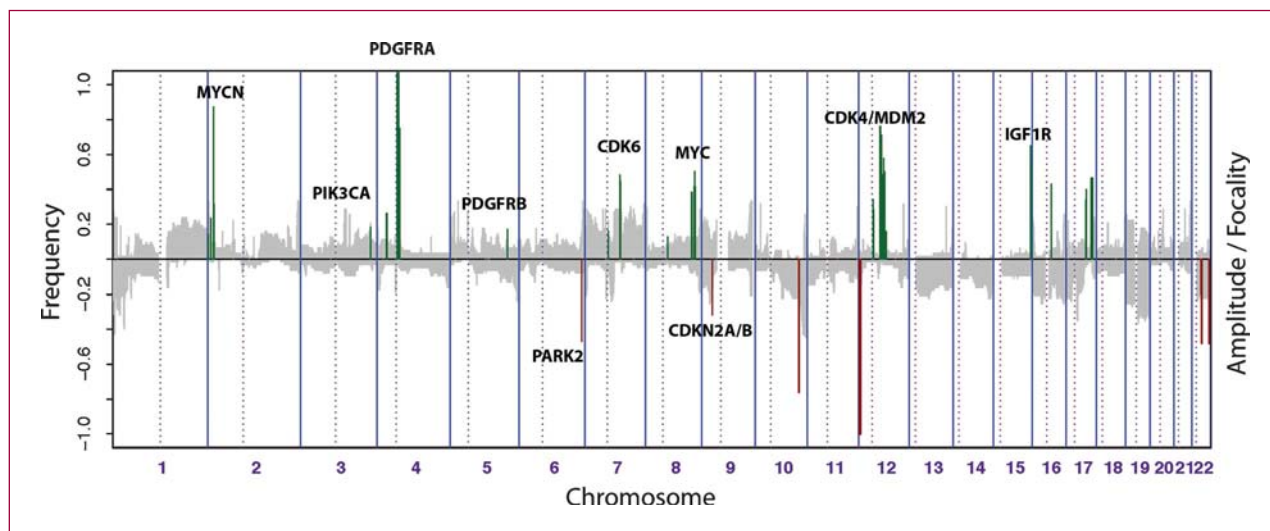
Fig. 3. Summary and significance of genomic aberrations in pediatric high-grade glioma. The proportion of tumors in which each clone is gained or lost is plotted in grey (*Y*-axis) for each BAC clone according to genomic location (*X*-axis). A measure of the frequency, amplitude, and focality of high-level events was calculated for each affected clone and was overplotted for amplifications (green) and deletions (red), scaled to the absolute maximum for each.

(*P* = 0.00214, log-rank test; Fig. 2). The aneuploid and re-arranged cases fell in between, and were representative of the survival characteristics of the cohort as a whole, suggesting that they may need to be considered together as falling between the extremes of the other two groups.

One of the defining features of pediatric high-grade glioma is the frequent gain of chromosome 1q (12 of 63, or 19.0%, versus 17 of 189, or 9.0%, of adult cases; ref. 1; *P* = 0.039, Fisher's exact test) and loss of 16q (11 of 63, or 17.5%, versus 14 of 189, of 7.4%; *P* = 0.028, Fisher's exact test); in contrast to adult glioblastoma cases, in which gains of chromosome 7 (12 of 63, or 19.0%, versus 140 of 189, or 74.1%; *P* < 0.0001, Fisher's exact test) and losses of 10q (10 of 63, or 15.9%, versus 152 of 189, or 80.4%; *P* < 0.0001, Fisher's exact test) predominate. In our FFPE cohort, we noticed a clear distinction of 1q gain cases from those with concurrent 7 gain/10q loss (7+/10q-, 8 of 63, or 12.7%), with only a single case harboring both abnormalities. Neither event was significantly associated with any clinicopathologic parameters, although there was a trend towards shorter survival in the 1q+ cases (*P* = 0.0865, log-rank test). Neither abnormality was seen in any infant cases.

Mapping of focal amplifications and deletions to known oncogenes and novel loci

As we had with large-scale alterations, we observed numerous focal amplifications and deletions. In summary, we identified 47 unique amplification and 32 unique deletions. All these events are detailed in full in Supplementary Table S2 (amplifications) and Supplementary Table S3 (deletions).

The most common amplicon was at 4q12 (10 of 63, or 15.9%), and deletion at 9p21 (10 of 63, or 15.9%, consisting of 8 homozygous, 2 hemizygous). Mapping the SRO in these cases narrowed these regions specifically to

PDGFRA and *CDKN2A*, respectively, confirming the initial observations that these are by far the most common amplifications/deletions in pediatric high-grade glioma (12). Other common events included amplification of *MYCN* at 2p24 (3 of 63, or 4.7%) or *MYC* at 8q24 (2 of 63, or 3.2%), together giving a frequency of 7.9% (5 of 63) of cases with genomic MYC family dysregulation; and 3 of 63 (4.7%) *EGFR* amplification at 7p12 – a lower frequency than observed in our recent chromogenic *in situ* hybridization study of a larger cohort of which this series is a subset, reflecting the focal nature of the amplification event in a small number of tumors identified by molecular pathology (19).

For the remaining aberrations, we highlighted the SROs where they were found to be recurrent. However, as most were present only in a single case, and we were unable to narrow down gained/lost regions, the result was that we identified a total of 1,026 amplified and 1,243 deleted genes across our series. To facilitate the identification of key oncogenic events in pediatric high-grade glioma, we sought to assign significance to the genomic aberrations we observed. Inspired by algorithms such as GISTIC (13) and GTS (16), we developed a simple measure based upon three key features of our data for each clone on the array: (*a*) frequency of high-level amplification/homozygous deletion, (*b*) absolute magnitude of the change, and (*c*) focality of the segmented copy number change. This amplitude/focality measure was then scaled to the maximum and minimum for amplifications/deletions, respectively, and plotted over the frequency of low-level gains and losses on the same histogram (Fig. 3).

As well as *PDGFRA* (the highest scoring gene) and *CDKN2A*, this analysis highlighted the importance of several known oncogenes, amplified at low frequency in our series, but at high magnitude, and in a focally restricted

manner. These included *PIK3CA* (3q26), *CDK6* (7q21), and *CDK4* (12q14), the first two previously reported in adult glioblastoma, but not in pediatric cases, and present here in a single case. We also identified amplifications of two additional receptor tyrosine kinases: *IGF1R* at 15q26 (Fig. 4A) and *PDGFRB* at 5q33 (Fig. 4B). Such an approach further highlighted the potential significance of known deletions targeting *PARK2* at 6q6 and *MGMT*, *PTPRE*, and others at 10q26, as well as unique events for which the candidate gene is unknown at 10q25 (Fig. 4C) and 11q14 (Fig. 4D).

We were able to validate nine of these lower-frequency amplification events by carrying out FISH on our FFPE sections using specific probes against *MYCN*, *PIK3CA*, *PDGFRA*, *SKP2*, *PDGFRB*, *MYC*, *CDK4*, *MDM2*, and *IGF1R* (Fig. 5).

Glioblastoma core signaling pathways are not commonly activated by copy number changes in pediatric patients

One of the most important findings from recent large-scale genomic profiling studies of adult glioblastoma was the identification of three core signaling pathways that were abrogated by amplification, deletion, and/or mutations of key genes in the vast majority of cases. Considering only the copy number data from these studies, 59%, 70%, and 66% of cases were found to have at least one genetic event targeting the receptor tyrosine kinase/phosphoinositide 3-kinase (RTK/PI3K), p53, or RB pathways, respectively (1, 2).

We mapped the copy number changes in our pediatric cases to the same pathways, which included many of the genes described above, as well as others described in adult
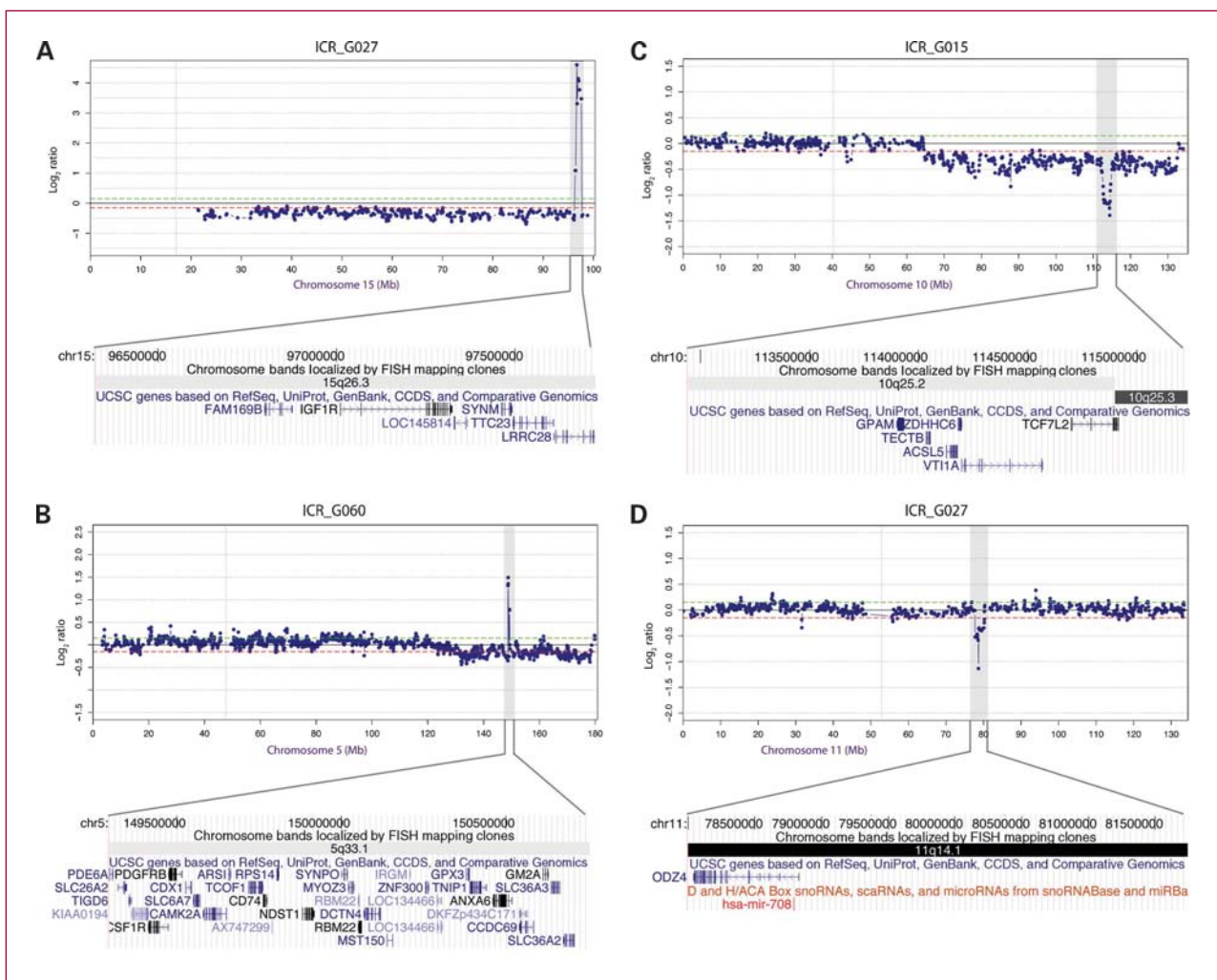

Fig. 4. Novel low-frequency amplifications and fine-mapping focal deletions in pediatric high-grade glioma. Chromosome plots for chromosome 15, targeting *IGF1R* (A); chromosome 5, targeting *PDGFRB/CSF1R* (B); chromosome 10, mapping a deletion at 10q25.2-q25.3 (C); and chromosome 11, resolving a deletion at 11q14 to *ODZ4* and hsa-mir-708 (D). Log$_2$ ratios for each clone are plotted (*Y*-axis) for each BAC clone according to location (*X*-axis) along the length of the chromosome, with genes and microRNA within the minimal regions plotted underneath according to positional information from the UCSC Genome Browser (hg18).
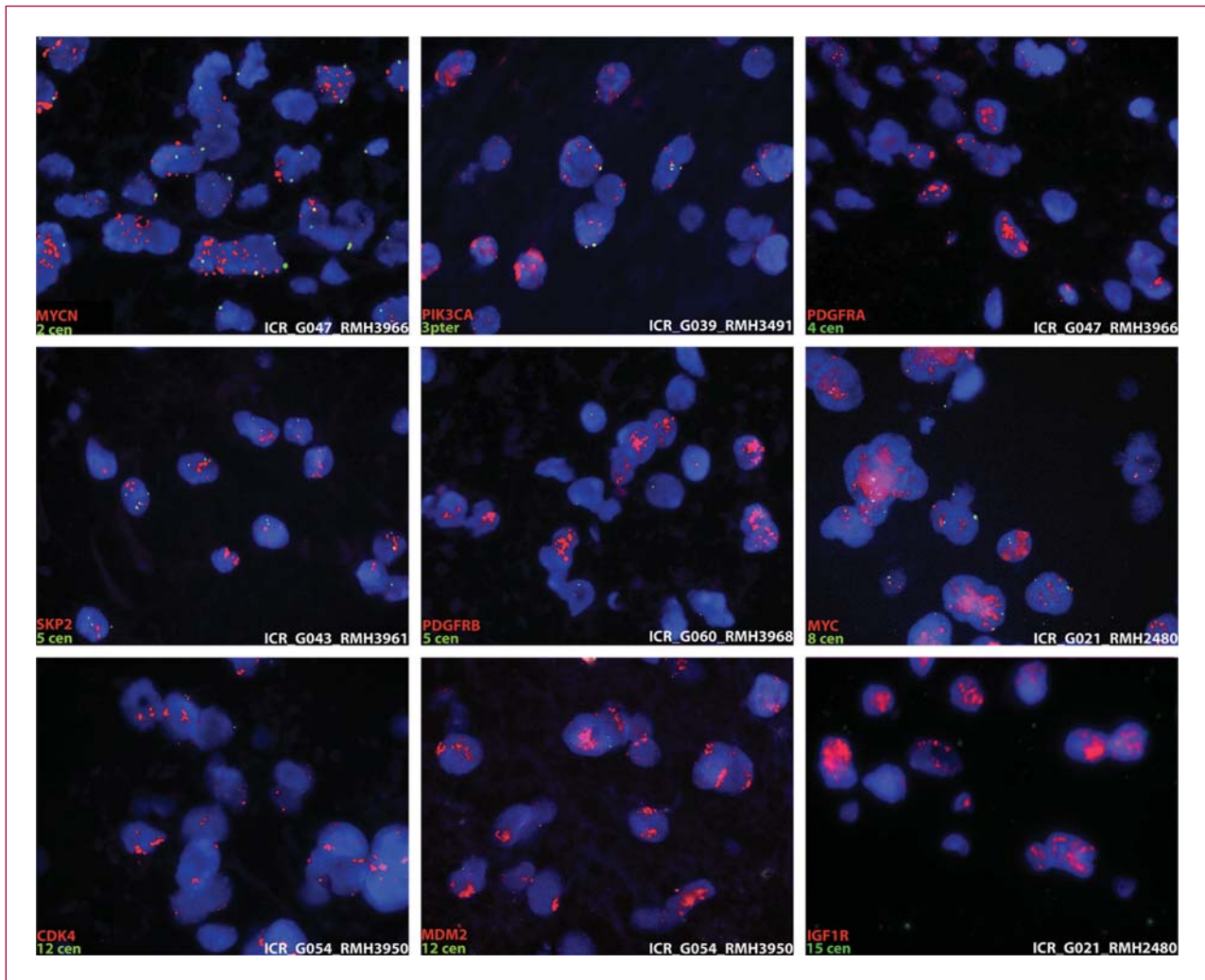
Fig. 5. FISH validation of low-frequency amplifications in pediatric high-grade glioma. Specific probes for *MYCN, PIK3CA, PDGFRA, SKP2, PDGFRB, MYC, CDK4, MDM2,* and *IGF1R* were labeled with Cy3 (red) and cohybridized to interphase nuclei on FFPE specimens with chromosome-specific control probes labeled with fluoroscein.

glioblastoma, including *MET, KRAS,* and *AKT2* (RTK/ PI3K), *MDM2* (p53), and *CCND2* (RB). Despite this, we observed a significantly lower frequency of pathway dysregulation compared with that reported in adults: 16 of 63 (25%) RTK/PI3K, 12 of 63 (19%) p53, and 14 of 63 (22%) RB (all $P < 0.0001$, Fisher's exact test; Fig. 6). Even after removing the stable genome subtype from this analysis, it is apparent that pediatric tumors show targeting of these core pathways by copy number alterations in less than half as many instances than in adults.

To explore whether other canonical pathways may be activated by this mechanism preferentially in childhood tumors, we mapped amplified/deleted genes in those tumors without core pathway targeting via GenMAPP. Although there were isolated cases with clear genomic events linked to activation of the Sonic Hedgehog (*GLI2* amplification, *HHIP* deletion) and Notch (*DLL3* amplification, *DLK1* deletion)

pathway activation, there was no consistently targeted pathway in these cases, nor was there specific enrichment of any additional pathway across the entire cohort.

Discussion

We were previously part of a collaborative study setting out to comprehensively map the copy number alterations present in the pediatric high-grade glioma genome, in which we used Affymetrix 500K SNP arrays on a series of 78 cases available as frozen tumor samples (12). Those data revealed an overlapping, but distinct, underlying molecular genetics of the childhood disease when compared with recent large-scale genomic analyses of adult high-grade glioma (1, 2). Along with the common amplification/deletion targets of *PDGFRA* and *CDKN2A/B,* there were numerous low-frequency events targeting both well-recognized

oncogenes and novel loci. The present study had three purposes: (*a*) to validate the high-frequency events in an independent set of samples, analyzed on an independent microarray platform; (*b*) to extend the sample set to provide evidence of recurrence of the low-frequency events previously reported; and (*c*) to identify novel low-frequency events, which by their nature may have been missed in the earlier study.

The most frequent focal events were *PDGFRA* amplification and *CDKN2A/B* deletion, and the most common large-scale gains and losses included chromosomes 1q and 16q, respectively. The $PDGFRA^{amp}$, 1q+, 16q- events were signifi-

cantly more common in the childhood setting (10, 11, 20), although it is important to note that they are present in a proportion of adult tumors. Similarly, we observed a group of tumors in our cohort containing aberrations more commonly associated with the adult disease, namely $EGFR^{amp}$, 7+, 10q-, albeit at significantly reduced frequencies. That they tended towards exclusivity suggests they represent archetypes for different ends of the spectrum of the disease.

One of the most intriguing differences observed in the pediatric setting was the presence of a proportion of cases of high-grade tumors with very few, or even no detectable copy number alterations. This was true on both BAC
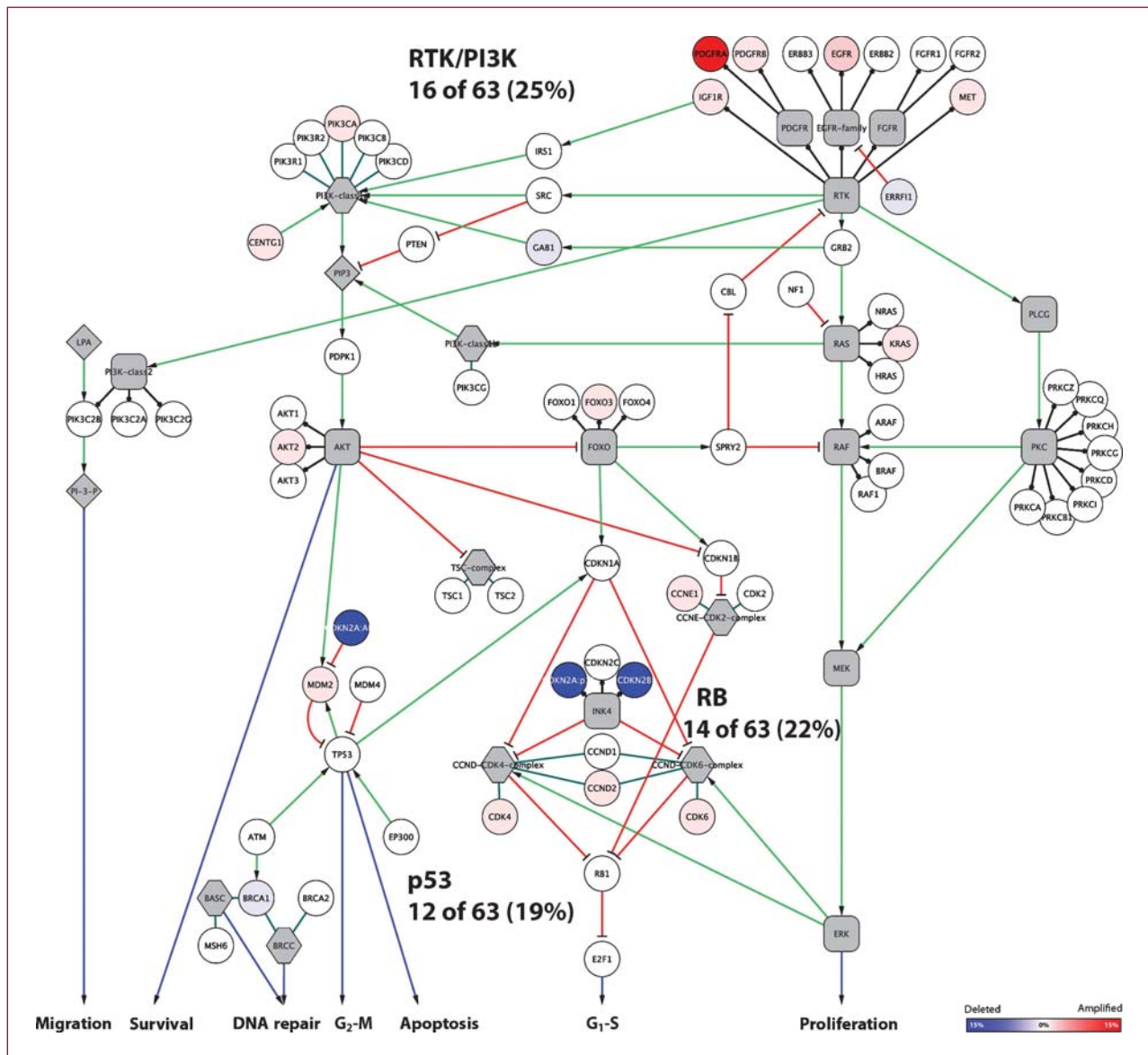

Fig. 6. Glioblastoma core signaling pathways are dysregulated by copy number changes less frequently in pediatric than in adult tumors. Signaling pathway heatmap of interactions defined by the cancer genome atlas (1). Red, genes with amplifications; blue, genes with focal deletion. The overall frequency of copy number alteration in pediatric high-grade glioma for each pathway is listed, and is significantly lower than in adults (25% RTK/PI3K, 19% p53, and 22% RB versus 59%, 70%, and 66% for adult glioblastoma, respectively).

(approximately 32,000 probes, 100 kb resolution) and SNP (approximately 500,000 probes, 6 kb resolution) platforms (12), and is in direct contrast to data from adult tumors (1, 2). This stable genomic profile is independent of histologic grade or type, and seems to convey an improved survival in patients with high-grade glioma, in contrast to those patients with an amplifier genomic profile, who do significantly worse.

Another of the defining features of the pediatric high-grade glioma genome is the numerous low-frequency amplifications and deletions present only in isolated cases in any given study. By nearly doubling the number of these rare tumors for which we have genomic data, we have been able to ascertain aberrations as recurrent across 132 cases. These include amplifications of known oncogenes within the core signaling pathways described in adult glioblastoma, such as *CDK6* (10), *MET*, and *CCND2*, as well as novel targets. These include *ID2* at 2p25, previously found in association with the *MYCN* amplicon at 2p24, possibly part of a single event, identified here as an independent target in its own right. ID2 is a helix-loop-helix transcription factor that has previously been shown to be widely expressed in astrocytic tumors (21, 22), and may play a role in negatively regulating cell differentiation and promoting cell survival (23, 24). Another amplicon at 17q22 was also confirmed in the FFPE series, with a SRO analysis identifying *RNF43* as the most likely target. RNF43 is a ubiquitin ligase that promotes cell growth and is upregulated in colon cancer (25, 26), but has not previously been implicated in gliomagenesis.

Homozygous deletions now apparent as recurrent lesions include those at 14q32, encompassing a large number of microRNAs, as well as the gene *DLK1*. DLK1 is a δ-like homolog that acts to inhibit Notch signaling through specific binding interactions with the receptor (27), and may play diverse roles in cellular transformation and differentiation (28). Although we have now observed two cases of homozygous deletion, other mechanisms of downregulation may be active, as *DLK1* is present at an imprinted locus, with increased methylation upstream of *GTL2* leading to reduced expression in other tumor types (29). Other deletions may have a more complicated role in gliomagenesis such as those on chromosome 16q. The SNP study identified a large deletion in a single tumor that is present as two separate events at 16q12 and 16q21 in two independent cases here, targeting numerous candidates including clusters of Iroquois homeobox genes, metallothioneins, and coiled-coil domain containing genes. By contrast, a homozygous deletion observed in the present study overlaps two independent loci previously reported at 11q14 to target a single microRNA, hsa-mir-708, and a single gene, *ODZ4*. Although little seems known about mir-708, the odd Oz/ten-m homolog 4 is expressed in the developing and adult central nervous system, and seems to act as an important transcriptional regulator associated with neurodevelopment (30, 31).

Finally, we were also able to identify several novel amplifications and deletions, the significance of many of which is not yet clear. There were some genes identified that were also present in adult glioblastoma studies which had not previously been reported in pediatric high-grade glioma, such as *AKT2*, *CCNE1*, *GLI2*, *MDM2*, *PARK2*, and *PIK3CA*. There were other previously unreported genes that may be associated with specific glioblastoma- related signaling pathways such as AKTIP (16q12), an Akt-interacting protein that acts as an activator of the PI3K pathway (32), and *PIK3C3* (18q12), also known as Vps34, a member of the PI3K family associated with autophagy (33). There were numerous others with potential functional relevance unknown.

We also noted rare amplifications at receptor tyrosine kinases considered less likely to be driven by copy number gain. Firstly was a very high level gain of *IGF1R* at 15q26 (11). Insulin-like growth factor (IGF) signaling has previously been implicated in gliomagenesis, primarily on the basis of high levels of the ligand *IGF2* in glioblastoma specimens (34). The growth-promoting effects of IGF2 that were shown were mediated via IGF1R and the PI3K regulatory subunit PIK3R3. Of particular relevance to the childhood setting was the observation of a mutual exclusivity between *IGF2*-associated tumors and *EGFR*-driven cases, suggesting that the IGF pathway may play a prominent role in pediatric tumors, possibly in concert with PDGF receptor (PDGFR)-related signaling.

Secondly was an amplicon at 5q33 which included *PDGFRB* (and another receptor tyrosine kinase *CSF1R*). Given the clear importance of PDGFR signaling on pediatric high-grade gliomas, it is perhaps unsurprising that there may be multiple mechanisms active in driving tumorigenesis through a common pathway. To this end, we also observed recurrent amplification of the ligand *PDGFB* (22q13) in the previous SNP study (12), and here further observed focal copy number gain at 7p22 encompassing *PDGFA*. That these unique genomic events have thus far been found to be restricted to pediatric tumors adds further evidence to a distinct underlying genetics driving archetypal high-grade gliomas in children, one that is largely PDGF-driven, and forms a discrete pole within the diversity of glioma biology. Understanding the most appropriate ways of efficaciously targeting these pathways in the most appropriate patient populations will hopefully overcome the disappointing early-phase clinical trials observed thus far with PDGFR inhibitors.

Disclosure of Potential Conflicts of Interest

Grant Support

References

1. McLendon R, Friedman A, Bigner D, et al. Comprehensive genomic characterization defines human glioblastoma genes and core pathways. Nature 2008;455:1061–8.

2. Parsons DW, Jones S, Zhang X, et al. An integrated genomic analysis of human glioblastoma multiforme. Science 2008;321:1807–12.

3. Rao SK, Edwards J, Joshi AD, Siu IM, Riggins GJ. A survey of glioblastoma genomic amplifications and deletions. J Neurooncol 2010; 96:169–79.

4. Gardina PJ, Lo KC, Lee W, Cowell JK, Turpaz Y. Ploidy status and copy number aberrations in primary glioblastomas defined by integrated analysis of allelic ratios, signal ratios and loss of heterozygosity using 500K SNP Mapping Arrays. BMC Genomics 2008;9:489.

5. de Tayrac M, Etcheverry A, Aubry M, et al. Integrative genome-wide analysis reveals a robust genomic glioblastoma signature associated with copy number driving changes in gene expression. Genes Chromosomes Cancer 2009;48:55–68.

6. Ruano Y, Mollejo M, Ribalta T, et al. Identification of novel candidate target genes in amplicons of Glioblastoma multiforme tumors detected by expression and CGH microarray profiling. Mol Cancer 2006;5:39.

7. Korshunov A, Sycheva R, Golanov A. Genetically distinct and clinically relevant subtypes of glioblastoma defined by array-based comparative genomic hybridization (array-CGH). Acta Neuropathol 2006; 111:465–74.

8. Rickert CH, Strater R, Kaatsch P, et al. Pediatric high-grade astrocytomas show chromosomal imbalances distinct from adult cases. Am J Pathol 2001;158:1525–32.

9. Wong KK, Tsang YT, Chang YM, et al. Genome-wide allelic imbalance analysis of pediatric gliomas by single nucleotide polymorphic allele array. Cancer Res 2006;66:11172–8.

10. Qu HQ, Jacob K, Fatet S, et al. Genome-wide profiling using single-nucleotide polymorphism arrays identifies novel chromosomal imbalances in pediatric glioblastomas. Neuro-oncol 2010;12:153–63.

11. Schiffman JD, Hodgson JG, VandenBerg SR, et al. Oncogenic BRAF mutation with CDKN2A inactivation is characteristic of a subset of pediatric malignant astrocytomas. Cancer Res 2010;70:512–9.

12. Paugh BS, Qu C, Jones C, et al. Integrated molecular profiling of pediatric high grade gliomas reveals key differences with the adult disease. J Clin Oncol 2010 May 17.

13. Beroukhim R, Getz G, Nghiemphu L, et al. Assessing the significance of chromosomal aberrations in cancer: methodology and application to glioma. Proc Natl Acad Sci U S A 2007;104:20007–12.

14. Maher EA, Brennan C, Wen PY, et al. Marked genomic differences characterize primary and secondary glioblastoma subtypes and identify two distinct molecular and clinical secondary glioblastoma entities. Cancer Res 2006;66:11502–13.

15. Natrajan R, Williams RD, Hing SN, et al. Array CGH profiling of favourable histology Wilms tumours reveals novel gains and losses associated with relapse. J Pathol 2006;210:49–58.

16. Wiedemeyer R, Brennan C, Heffernan TP, et al. Feedback circuit among INK4 tumor suppressors constrains human glioblastoma development. Cancer Cell 2008;13:355–64.

17. Lambros MB, Simpson PT, Jones C, et al. Unlocking pathology archives for molecular genetic studies: a reliable method to generate probes for chromogenic and fluorescent in situ hybridization. Lab Invest 2006;86:398–408.

18. Vuononvirta R, Sebire NJ, Dallosso AR, et al. Perilobar nephrogenic rests are nonobligate molecular genetic precursor lesions of insulin-like growth factor-II-associated Wilms tumors. Clin Cancer Res 2008; 14:7635–44.

19. Bax DA, Gaspar N, Little SE, et al. EGFRvIII deletion mutations in pediatric high-grade glioma and response to targeted therapy in pediatric glioma cell lines. Clin Cancer Res 2009;15:5753–61.

20. Zarghooni M, Bartels U, Lee E, et al. Whole-genome profiling of pediatric diffuse intrinsic pontine gliomas highlights platelet-derived growth factor receptor {α} and poly (ADP-ribose) polymerase as potential therapeutic targets. J Clin Oncol 2010;28:1337–44.

21. Mikami S, Hirose Y, Yoshida K, et al. Predominant expression of OLIG2 over ID2 in oligodendroglial tumors. Virchows Arch 2007; 450:575–84.

22. Vandeputte DA, Troost D, Leenstra S, et al. Expression and distribution of id helix-loop-helix proteins in human astrocytic tumors. Glia 2002;38:329–38.

23. Gray MJ, Dallas NA, Van Buren G, et al. Therapeutic targeting of Id2 reduces growth of human colorectal carcinoma in the murine liver. Oncogene 2008;27:7192–200.

24. Obayashi S, Tabunoki H, Kim SU, Satoh J. Gene expression profiling of human neural progenitor cells following the serum-induced astrocyte differentiation. Cell Mol Neurobiol 2009;29:423–38.

25. Sugiura T, Yamaguchi A, Miyamoto K. A cancer-associated RING finger protein, RNF43, is a ubiquitin ligase that interacts with a nuclear protein, HAP95. Exp Cell Res 2008;314:1519–28.

26. Yagyu R, Furukawa Y, Lin YM, Shimokawa T, Yamamura T, Nakamura Y. A novel oncoprotein RNF43 functions in an autocrine manner in colorectal cancer. Int J Oncol 2004;25:1343–8.

27. Nueda ML, Baladron V, Sanchez-Solana B, Ballesteros MA, Laborda J. The EGF-like protein dlk1 inhibits notch signaling and potentiates adipogenesis of mesenchymal cells. J Mol Biol 2007;367: 1281–93.

28. Espina AG, Mendez-Vidal C, Moreno-Mateos MA, et al. Induction of Dlk1 by PTTG1 inhibits adipocyte differentiation and correlates with malignant transformation. Mol Biol Cell 2009;20:3353–62.

29. Kawakami T, Chano T, Minami K, Okabe H, Okada Y, Okamoto K. Imprinted DLK1 is a putative tumor suppressor gene and inactivated by epimutation at the region upstream of GTL2 in human renal cell carcinoma. Hum Mol Genet 2006;15:821–30.

30. Tucker RP, Chiquet-Ehrismann R. Teneurins: a conserved family of transmembrane proteins involved in intercellular signaling during development. Dev Biol 2006;290:237–45.

31. Zhou XH, Brandau O, Feng K, et al. The murine Ten-m/Odz genes show distinct but overlapping expression patterns during development and in adult brain. Gene Expr Patterns 2003;3:397–405.

32. Remy I, Michnick SW. Regulation of apoptosis by the Ft1 protein, a new modulator of protein kinase B/Akt. Mol Cell Biol 2004;24: 1493–504.

33. Simonsen A, Tooze SA. Coordination of membrane events during autophagy by multiple class III PI3-kinase complexes. J Cell Biol 2009;186:773–82.

34. Soroceanu L, Kharbanda S, Chen R, et al. Identification of IGF2 signaling through phosphoinositide-3-kinase regulatory subunit 3 as a growth-promoting axis in glioblastoma. Proc Natl Acad Sci U S A 2007;104:3466–71.

Clinical Cancer Research

A Distinct Spectrum of Copy Number Aberrations in Pediatric High-Grade Gliomas

Dorine A. Bax, Alan Mackay, Suzanne E. Little, et al.

Updated version	Access the most recent version of this article at: doi:10.1158/1078-0432.CCR-10-0438
Supplementary Material	Access the most recent supplemental material at: http://clincancerres.aacrjournals.org/content/suppl/2010/08/25/1078-0432.CCR-10-0438.DC1

Cited articles	This article cites 33 articles, 12 of which you can access for free at: http://clincancerres.aacrjournals.org/content/16/13/3368.full#ref-list-1
Citing articles	This article has been cited by 9 HighWire-hosted articles. Access the articles at: http://clincancerres.aacrjournals.org/content/16/13/3368.full#related-urls

E-mail alerts	Sign up to receive free email-alerts related to this article or journal.
Reprints and Subscriptions	To order reprints of this article or to subscribe to the journal, contact the AACR Publications Department at pubs@aacr.org.
Permissions	To request permission to re-use all or part of this article, use this link http://clincancerres.aacrjournals.org/content/16/13/3368. Click on "Request Permissions" which will take you to the Copyright Clearance Center's (CCC) Rightslink site.